

Thermal Conductivity and Elastic Modulus Evolution of Thermal Barrier Coatings under High Heat Flux Conditions

Dongming Zhu and Robert A. Miller

(Submitted 28 December 1998; in revised form 6 December 1999)

Laser high heat flux test approaches have been established to obtain critical properties of ceramic thermal barrier coatings (TBCs) under near-realistic temperature and thermal gradients that may be encountered in advanced engine systems. Thermal conductivity change kinetics of a thin ceramic coating were continuously monitored in real time at various test temperatures. A significant thermal conductivity increase was observed during the laser-simulated engine heat flux tests. For a 0.25 mm thick ZrO_2 -8% Y_2O_3 coating system, the overall thermal conductivity increased from the initial value of 1.0 W/m K to 1.15, 1.19, and 1.5 W/m K after 30 h of testing at surface temperatures of 990, 1100, and 1320 °C, respectively. Hardness and elastic modulus gradients across a 1.5 mm thick TBC system were also determined as a function of laser testing time using the laser sintering/creep and microindentation techniques. The coating Knoop hardness values increased from the initial hardness value of 4 GPa to 5 GPa near the ceramic/bond coat interface and to 7.5 GPa at the ceramic coating surface after 120 h of testing. The ceramic surface modulus increased from an initial value of about 70 GPa to a final value of 125 GPa. The increase in thermal conductivity and the evolution of significant hardness and modulus gradients in the TBC systems are attributed to sintering-induced microporosity gradients under the laser-imposed high thermal gradient conditions. The test techniques provide a viable means for obtaining coating data for use in design, development, stress modeling, and life prediction for various TBC applications.

Keywords thermal barrier coating, laser sintering and creep, thermal conductivity change kinetics, elastic modulus

1. Introduction

Ceramic thermal barrier coatings (TBCs) are being developed for advanced gas turbine engine components to improve engine efficiency and reliability. However, the durability of the coating systems remains a crucial issue under the conditions of increased operating temperature and extended hot exposure time that will be encountered in next generation engines. In particular, changes in thermomechanical and thermophysical properties as a result of coating sintering, such as the increase in coating elastic modulus and thermal conductivity, have become a major focal point in the development of advanced TBCs. Temperature-dependent change kinetics of the coating thermal conductivity and elastic modulus are among the most important parameters required for coating design and life prediction. Therefore, determination of thermal conductivity and elastic modulus evolution of TBCs under near-realistic engine temperature and thermal gradients is of great importance.

In this paper, a laser steady-state heat flux technique is established to monitor overall thermal conductivity of ceramic coatings under simulated engine temperature and heat load conditions. Thermal conductivity change kinetics are thus determined for a

plasma-sprayed ZrO_2 -8 wt.% Y_2O_3 coating under a given laser heat flux and various surface temperature conditions. The elastic modulus evolution across a ZrO_2 -8 wt.% Y_2O_3 ceramic coating is achieved by a laser pressure sintering and creep technique. The modulus change kinetics as a function of time and coating thickness are subsequently determined after the laser sintering experiments using the Knoop microindentation approach.

2. Experimental Materials and Methods

2.1 Thermal Conductivity Change Kinetics by Laser Steady-State Heat Flux Technique

A high power CO_2 laser was used to investigate thermal conductivity change kinetics of the ceramic coating under steady-state heating conditions. Figure 1(a) shows a schematic diagram of the laser test rig. This rig consists of a 3.0 kW CO_2 continuous wave laser (wavelength 10.6 μm) (EVERLASE Vulcan, Coherent General Inc., Sturbridge, MA), a motor-driven rotating test station, and temperature measurement instruments such as a thermograph system and pyrometers. The specimen configuration used for the thermal conductivity study was the 25.4 mm diameter, 3.2 mm thick CMSX-4 single-crystal superalloy substrate, coated with a 0.12 mm low-pressure plasma-sprayed (LPPS) Ni-36Cr-5Al-Y bond coat and a 0.25 mm air plasma-sprayed (APS) ZrO_2 -8 wt.% Y_2O_3 ceramic coating. The specimen surface heating was provided by the laser beam, and the backside air cooling was used to maintain the desired specimen temperatures. A 12.5 mm thick aluminum plate with a 23.9 mm diameter center hole opening was used as an aperture to prevent the specimen from edge or side heating. A uniform laser power distribution was

Dongming Zhu, Ohio Aerospace Institute, National Aeronautics and Space Administration, Glenn Research Center; and **Robert A. Miller**, National Aeronautics and Space Administration, Glenn Research Center, Cleveland, OH 44135. E-mail: Dongming.Zhu@grc.nasa.gov

achieved over a 23.9 mm diameter aperture region of the specimen (as confirmed by thermograph) by using an integrating ZnSe lens combined with the specimen rotation. Three platinum wire (wire diameter 0.38 mm) flat coils were used to form an air gap between the aluminum aperture plate and the specimen to minimize the specimen heat losses through the plate.

During the thermal conductivity change kinetics testing, the ceramic surface temperature was measured by an 8 μm infrared pyrometer (Model MX-M803 Maxline Infrared Thermometer Measurement and Control System, Ircon, Inc., Niles, IL). A side hole with diameter 1.06 mm (shown in Fig. 1) was drilled through the center of the substrate by the electrodischarge machining (EDM) method, and the metal temperature at the midpoint of substrate thickness near the center region was determined by an embedded type K thermocouple (1 mm diameter Inconel alloy

sheathed thermocouple, Omega Engineering, Inc., Stamford, CT). Using the reported thermal conductivity values of the CMSX-4 metal substrate^[1] and a similar bond coat^[2] shown in Fig. 2, and the initial thermal conductivity 1.0 W/m K for the ZrO_2 -8 wt.% Y_2O_3 ,^[3] the interfacial temperatures, and thus the actual heat flux passing through the TBC system, were determined under the steady-state laser heating conditions by one-dimensional (1-D) heat transfer models.^[4] The radiation heat loss (total emissivity was taken as 0.50^[5,6]) and laser absorption corrections of the ceramic coating were considered in the calculations. Therefore, overall thermal conductivity changes were continuously monitored in real time during the test period by measuring the temperature difference across the ceramic coating. In the present study, three tests were carried out under the pass-through laser heat flux of 64 W/cm^2 . During the tests, the ceramic surface temperatures were maintained at approximately 990, 1100, and 1320°C, respectively. The total test time was up to 33 h for a single test.

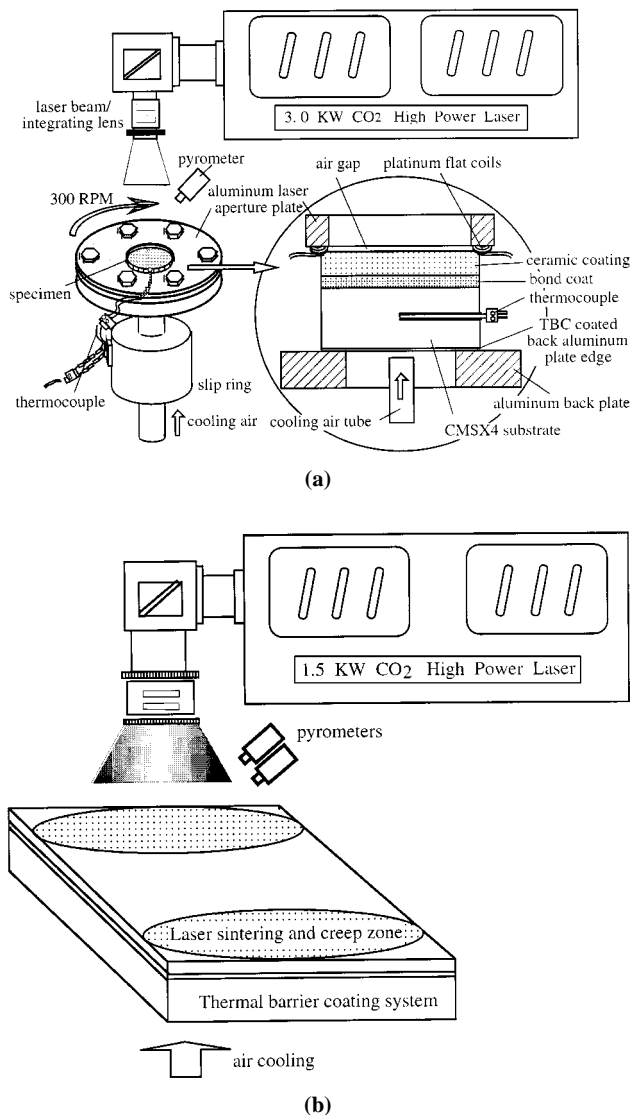


Fig. 1 Schematic diagrams of high power CO₂ laser rigs for determining thermal conductivity change kinetics and elastic modulus evolution of the ceramic TBCs under steady-state heat flux conditions. (a) Laser high heat flux technique for monitoring thermal conductivity change kinetics. (b) Laser sintering and creep technique for evaluating ceramic creep behavior and modulus evolution under thermal gradient conditions

2.2 Elastic Modulus Evolution under High Heat Flux Conditions

The laser sintering and creep tests were carried out to induce elastic modulus changes in the porous and microcracked TBC under high thermal gradients using a 1.5 kW CO₂ laser (EVER-LASE Arrow, Coherent General Inc., Sturbridge, CT), as shown in Fig. 1(b). The detailed laser test conditions and procedures have been described elsewhere.^[7] The specimen configuration used for the modulus study consisted of a 1.5 mm thick ZrO_2 -8 wt.% Y_2O_3 ceramic coating and a 0.25 mm thick Fe-25Cr-5Al-0.5Y bond coat, which were sprayed on the 4140 steel substrate (dimension 127 × 32 × 12.7 mm). During the laser sintering test, the ceramic surface temperature was maintained at about 1080 °C and the back side metal temperature at 100 °C. The specimens were continuously heated for either 1, 11, 22, and 120 h. The ceramic creep strains were measured from the through-thickness, wedge-shape crack openings in the ceramic coating that were observed both on the coating surface and in the cross sections by metallography after the laser sintering experiments.

The Knoop indentation method has been used to measure the elastic modulus of bulk ceramics^[8] and ceramic coatings.^[9,10] By measuring the elastic recovery of the residual surface impression

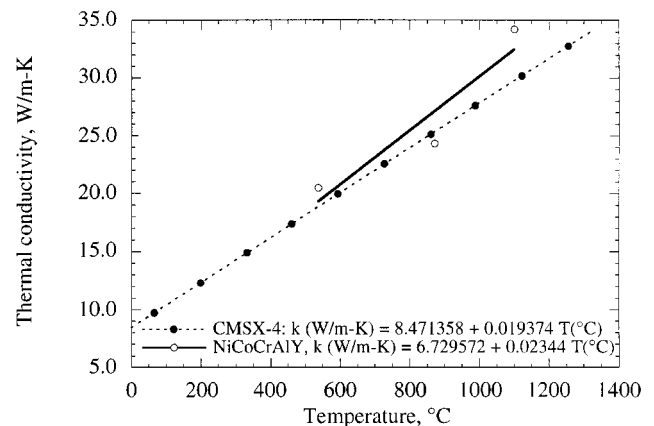


Fig. 2 Literature reported thermal conductivity values for the CMSX-4 metal substrate and NiCoCrAlY bond coat

of the indentation long and short diagonals (with half lengths a' and b' respectively) and hardness H , the modulus E can be estimated by

$$E = \alpha \cdot \left(\frac{b}{a} - \frac{b'}{a'} \right)^{-1} \cdot H = \alpha \cdot \left(\frac{b}{a} - \frac{b'}{a'} \right)^{-1} \cdot H \quad (\text{Eq 1})$$

where α is a constant ($\alpha = 0.45$), a and b are the half lengths of the long and short diagonals before elastic recovery, and $b/a = 1/7.11$ for a perfect indenter. In this study, the ceramic coating modulus distributions as a function of time were determined on the cross sections of the coating system after the laser sintering tests using this Knoop indentation technique. The Knoop indentation tests were carried out on the polished cross sections of laser-sintered specimens using a microhardness tester (Micromet II, Buehler, IL), in accordance with ASME C1326. The load used was 500 g (4.9 N) and the dwell time was 15 s. At least eight column indentation sequences (more than 150 measurements) across the coating system were performed for each specimen.

3. Experimental Results and Discussion

3.1 Thermal Conductivity Change Kinetics

Figure 3 shows typical temperature profiles of the ZrO_2 -8 wt.% Y_2O_3 TBC system tested at a surface temperature of approximately 1320 °C during the laser thermal conductivity test. Under the constant steady-state laser high heat flux condition (heat flux approximately 64 W/cm^2), the measured ceramic surface temperature slightly decreased with time. On the other hand, the measured metal temperature increased with time. The temperature difference across the ceramic layer decreased from approximately 140 °C at the initial stage to 110 °C after 33 h of testing, suggesting an overall thermal conductivity increase in the ceramic layer due to laser sintering. Note that a thermal conductivity gradient would be established across the ceramic coating (faster thermal conductivity increase near the ceramic surface as compared to near the ceramic/bond coat interface) under the high thermal gradient conditions. Therefore, the ceramic thermal conductivity increase in the coating determined by the steady-state laser heat flux approach will reflect an overall effect of the conductivity increase in the coating. Figure 4 shows the overall thermal conductivity change kinetics of the

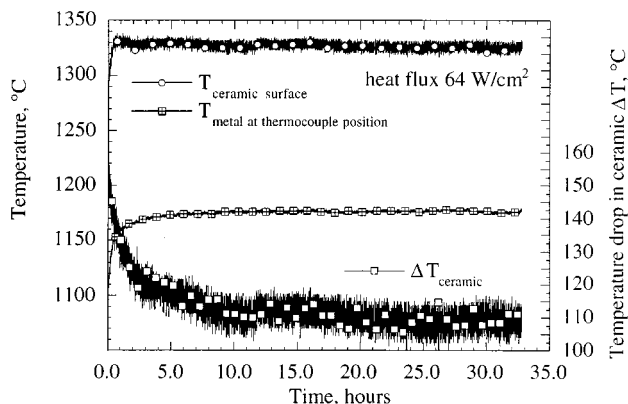


Fig. 3 Typical temperature profiles of the ZrO_2 -8 wt.% Y_2O_3 TBC system tested at a surface temperature of approximately 1320 °C during the laser thermal conductivity test

TBC determined by the real time laser heat flux testing. The thermal conductivity increased from the initial value of 1 $\text{W}/\text{m K}$ to 1.15, 1.19, and 1.5 $\text{W}/\text{m K}$ after 30 h of testing at the surface temperatures of 990, 1100, and 1320 °C, respectively. The thermal conductivity change kinetics also showed the distinct two-stage rate increase characteristics: a fast and changing rate conductivity increase at the initial “primary” stage, and a slower rate and nearly constant conductivity increase at the “steady-state” stage. The irreversible thermal conductivity increase was demonstrated in the 990 °C test where a couple of temperature cycles were introduced. The interrupted tests by thermal cycling did not alter the general trend of the thermal conductivity change kinetics.

Figure 5 illustrates the ceramic thermal conductivity $\ln(k)$ as a function of the Larson-Miller (L-M) parameter ($L-M = T[\ln(t) + C]$, where t is the heating time in seconds, T_{ave} is the average temperature in Kelvin in the ceramic coating and C is a fitting constant, equal to 10 in this study). The effects of heating time and temperature on the overall ceramic thermal conductivity are approximately described by the $\ln(k)$ versus L-M relationship.

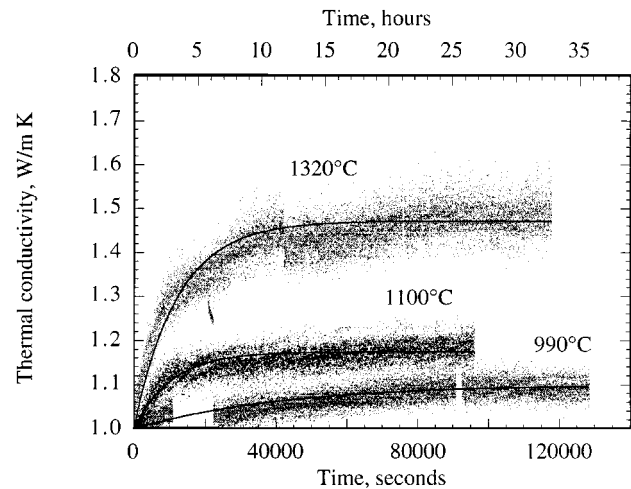


Fig. 4 The overall thermal conductivity change kinetics of the ZrO_2 - Y_2O_3 TBC determined by the real time laser heat flux testing

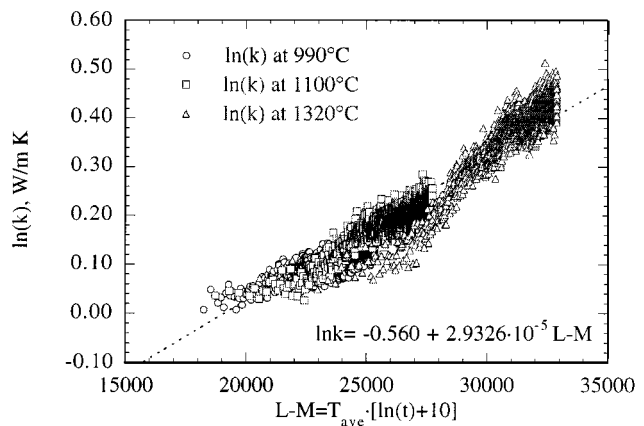
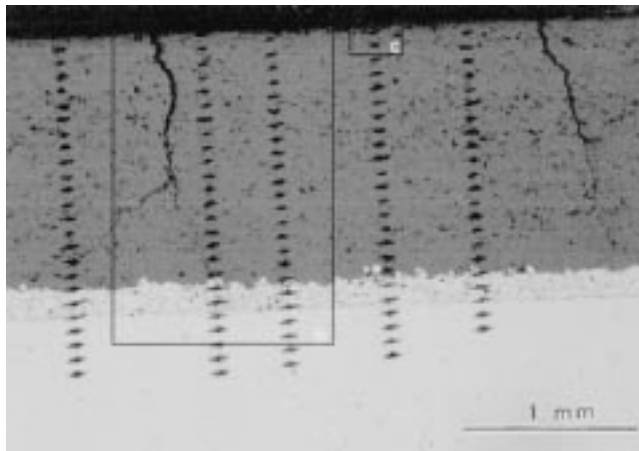
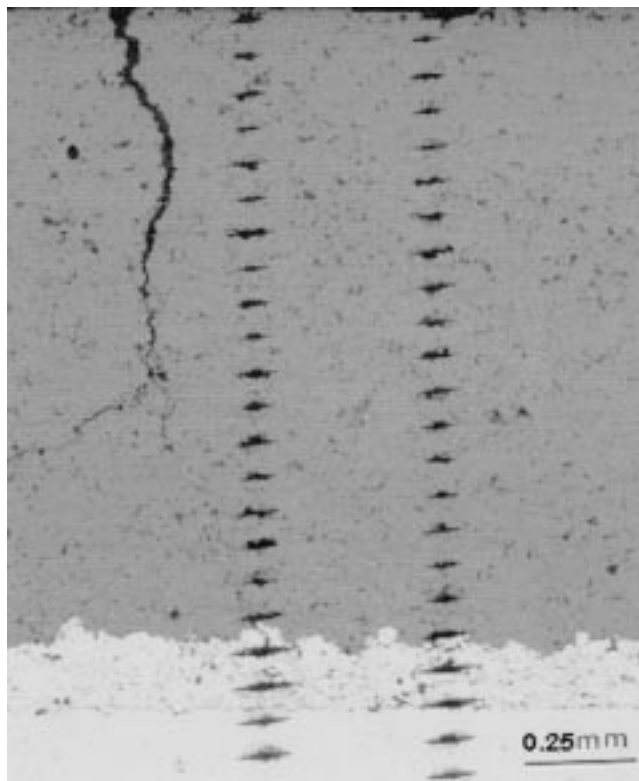


Fig. 5 Ceramic thermal conductivity $\ln(k)$ as a function of the L-M parameter ($L-M = T[\ln(t) + C]$, where t is the heating time in seconds, T is the absolute temperature in Kelvin, and C is a constant). The effects of heating time and temperature on the overall ceramic thermal conductivity are described by the conductivity - L-M relationship

The average slope of the L-M plot for the ZrO_2 -8 wt.% Y_2O_3 coating was about 2.93×10^{-5} for the TBC system. The L-M slope obtained in this study is slightly higher than the slopes reported in the literature.^[11,12] This discrepancy may be attributed to a significantly fast conductivity increase at the primary stage for the coating observed in this study. Note that the L-M extrapolation approach for the thermal conductivity change kinetics cannot accurately describe the fast, variable conductivity increase rate at the initial primary stage. An approach is being established to



(a)



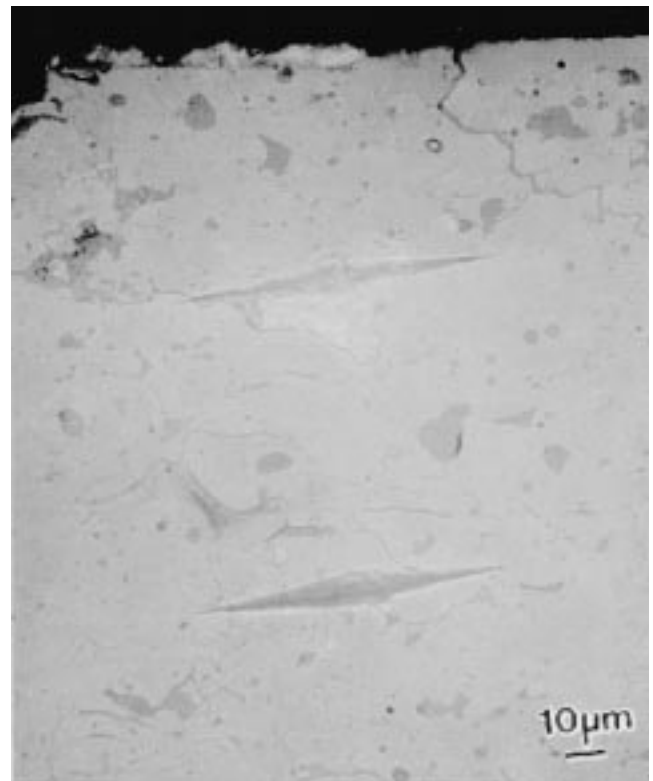
(b)

characterize the ceramic thermal conductivity increase kinetics and the conductivity gradient effect under high heat flux conditions based on the visco-elastic relaxation theory.^[4]

3.2 The Elastic Modulus Evolution of the Ceramic Coating

Figure 6 illustrates the micrographs of cross sections of the TBC and Knoop hardness indentations after an 11 h laser sintering and creep test. Note that through-thickness, wedge-shape cracks were developed in the ceramic coatings as a result of the laser sintering. The microporosity was reported to decrease with increasing laser testing time, and the microcrack density observed in the ceramic coating near the surface region was much lower than that near the ceramic/bond coat interface region after the laser testing.^[4] The porosity gradients across the coating thickness after laser testing were correlated to the measured total creep strain gradients shown in Fig. 7.^[4] The morphology change in the ceramic coating is expected to result in coating hardness and modulus increases with laser testing time.

Figure 8 illustrates Knoop hardness distributions in the ZrO_2 -8 wt.% Y_2O_3 TBC system after laser sintering for various times. The hardnesses of the FeCrAlY and the steel substrate were approximately 2 to 3 GPa and essentially unaffected during the testing. The ceramic coating showed higher hardness values as compared to the bond coat and substrate. Note that the coating hardness increases after the laser testing. It can be seen that after



(c)

Fig. 6 Micrographs of cross sections of the TBC and Knoop hardness indentations after 11 h of laser sintering and creep test (Fig. 6a through c show various magnifications of the coating system, respectively)

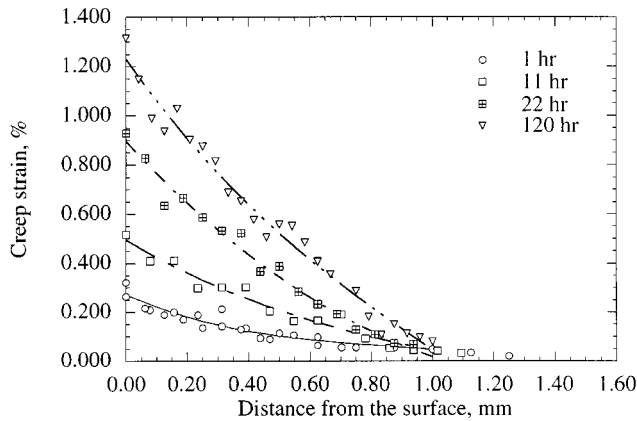


Fig. 7 The creep strain gradient resulting from laser-imposed temperature and stress gradients as a function of laser testing time in a ZrO_2 -8 wt.% Y_2O_3 TBC system

1 h of laser sintering, the increase in the coating hardness was relatively small, with coating hardness values in the range of 4 to 5 GPa, which were not much higher than the initial untested coating hardness value of about 4 GPa. However, after 11 h of laser sintering, the coating surface region had a significant increase in hardness (near surface hardness value of about 7 GPa), but the near ceramic/bond coat interface region remained almost unchanged. After 120 h of laser sintering, the entire ceramic coating had a more significant increase in hardness. The Knoop hardness values increased from the initial hardness value of 4 GPa to 5 GPa near the ceramic/bond coat interface and to 7.5 GPa at the ceramic coating surface.

Figure 9 shows the elastic modulus measurement results in the ZrO_2 -8 wt.% Y_2O_3 TBC obtained by the indentation technique as a function of laser sintering time. The relatively large data scatter in the modulus values is a consequence of the porous and heterogeneous nature of the plasma-sprayed ceramic coating. Therefore, the experimental data have been smoothed using a fifth-order polynomial. It can be seen that the ceramic modulus change followed a similar trend to the ceramic hardness change during the laser sintering process. The surface modulus increased from an initial value of about 70 GPa to the final value of 125 GPa, after 120 h of testing. The experimentally determined modulus change kinetics across the coating system shown in Figure 10 can be well described by the visco-elastic behavior:^[7]

$$\frac{E_c - E_c^0}{E_c^{\text{inf}} - E_c^0} = C_E \left\{ 1 - \exp \left[-\frac{t}{\tau} \right] \right\} \quad (\text{Eq 2})$$

where E_c is the coating modulus at any given time t ; E_c^0 and E_c^{inf} are ceramic coating modulus values at the initial time and at infinitely long time, respectively; τ is relaxation time; and C_E is a constant related to temperature and stress in the coating system. It can be seen that a modulus gradient was established in the coating system, which evolved with time under the laser-imposed temperature and stress gradients. The surface showed very fast modulus increase kinetics. The surface of the ceramic coating

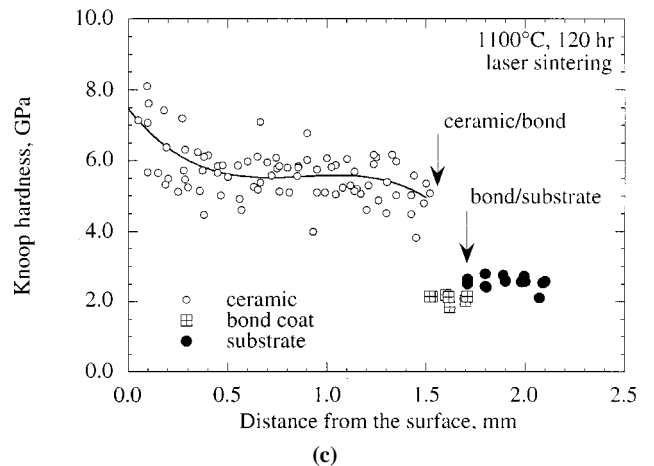
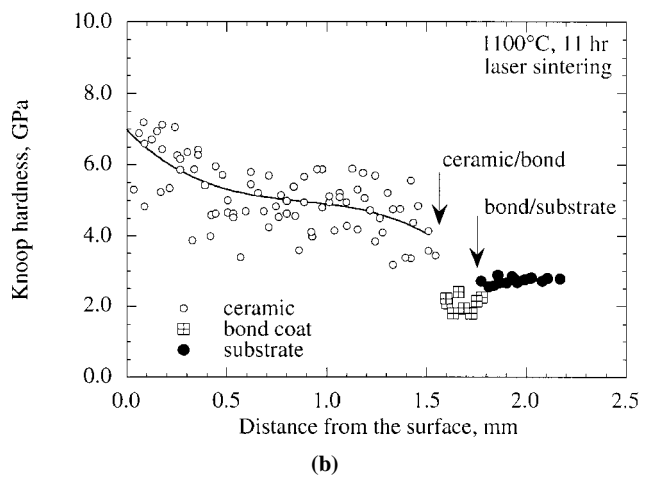
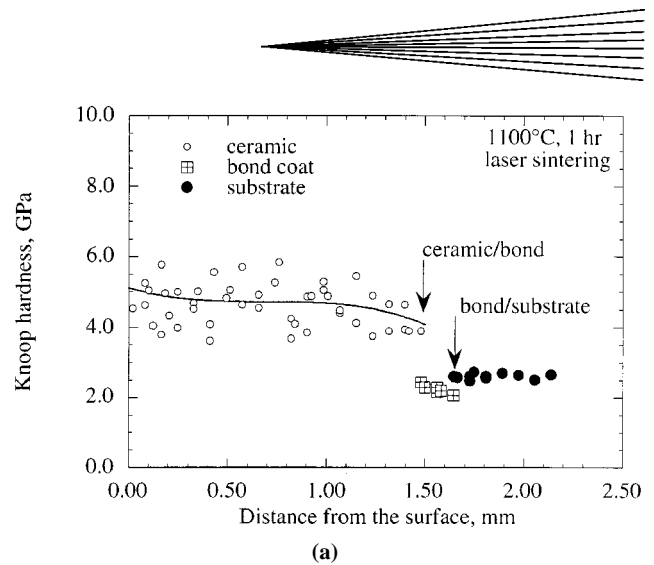


Fig. 8 Knoop hardness distributions in a ZrO_2 -8 wt.% Y_2O_3 TBC system after laser sintering for various times showing the significant hardness increase and hardness gradient development in the coating system: (a) 1 h, (b) 11 h, and (c) 120 h

reached nearly the assumed final modulus value of 125 GPa in about 20 h. However, from the experimental observations, a much longer time is required for the inner layers of the ceramic coating to obtain the final modulus value by laser sintering due

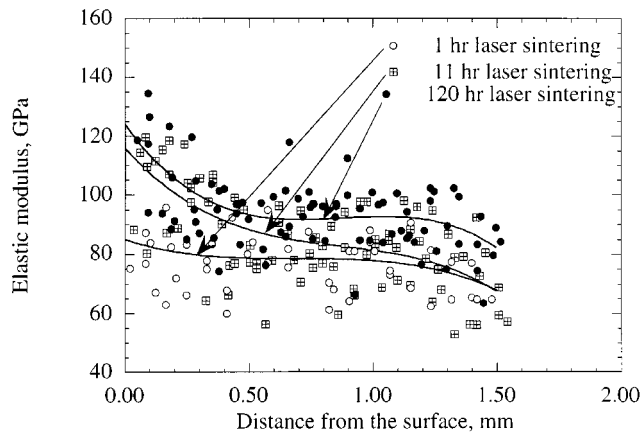


Fig. 9 The elastic modulus distributions in the ZrO₂-8 wt.% Y₂O₃ TBC as a function of laser sintering time

to the lower temperatures and stresses under the thermal gradient test conditions.

4. Concluding Remarks

High heat flux test approaches have been established to obtain critical properties of TBCs under near-realistic temperature and thermal gradients encountered in advanced engine systems. In particular, the laser steady-state technique provides a unique approach for quantitatively monitoring thermal conductivity change kinetics of the ceramic coating under high heat flux conditions. The laser sintering and creep technique offers an effective means for quantitatively evaluating ceramic creep behavior and modulus evolution under simulated engine conditions. The test techniques are important for coating design and development, stress modeling, and life prediction for various TBC applications.

A significant thermal conductivity increase was observed during the laser steady-state high heat flux testing. For a 0.25 mm ZrO₂-8 wt.% Y₂O₃ coating, the overall thermal conductivity increased from the initial value of 1 W/m K to 1.15, 1.19, and 1.5 W/m K after 30 h of testing at the surface temperatures of 990, 1100, and 1320 °C, respectively. The thermal conductivity change kinetics showed the distinguished two-stage rate increase characteristics: a fast and changing rate conductivity increase at the initial primary stage and a slower rate and nearly constant conductivity increase at the steady-state stage.

The microporosity was observed to decrease with increasing laser testing time during the laser sintering and creep test. The microporosity gradients, corresponding to the creep strain gradients across the coating thickness after laser testing, resulted in significant hardness and modulus gradients in the coating. The Knoop hardness values increased from the initial value of 4 GPa to 5 GPa near the ceramic/bond coat interface and to 7.5 GPa at the ceramic coating surface after 120 h of testing. During the same period of time, the surface modulus increased from an initial value of about 70 GPa to the final value of 125 GPa.

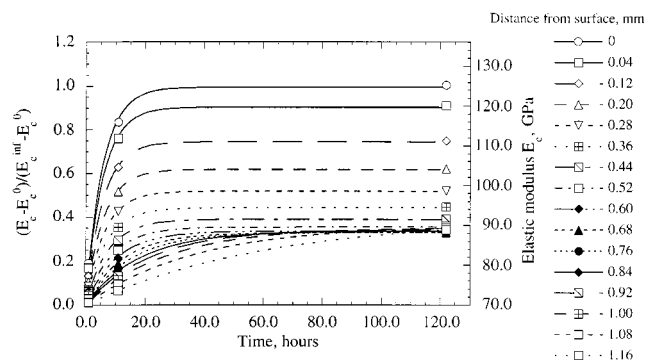


Fig. 10 The experimentally determined modulus change kinetics across the coating system under laser sintering and creep conditions

Acknowledgment

The authors are grateful to George W. Leissler, Dynacs Engineering Company, Inc., Lewis Group, for his assistance in the preparation of the TBCs.

References

1. "CMSX Property Data," Cannon-Muskegon Corporation, Muskegon, MI, 1994.
2. J.T. DeMasi, K.D. Sheffler, and M. Ortiz: "Thermal Barrier Coating Life Prediction Model Development: Phase I-Final Report," NASA CR-182230, NASA, Washington, DC, Dec. 1989.
3. R.A. Miller and G.W. Leissler: "Characterization and Durability Testing of Plasma-Sprayed Zirconia-Yttria and Hafnia-Yttria Thermal Barrier Coatings," NASA Technical Paper 3296, NASA, Washington, DC, Mar. 1993.
4. D. Zhu and R.A. Miller: "Determination of Thermal Conductivity Change Kinetics under Steady-State Laser Heat Flux Conditions," NASA Technical Memorandum, 209069, NASA, Washington, DC, 1999.
5. C.H. Liebert: "Emittance and Absorptance of NASA Ceramic Thermal Barrier Coating System," NASA Technical Paper TP-1190, NASA, Washington, DC, 1978.
6. C.H. Liebert: "Emittance and Absorptance of the National Aeronautics and Space Administration Ceramic Thermal Barrier Coating," *Thin Solid Films*, 1978, vol. 53, pp. 235–40.
7. D. Zhu and R.A. Miller: "Determination of Creep Behavior of Thermal Barrier Coatings under Laser Imposed Temperature and Stress Gradients," NASA Technical Memorandum 113169, Army Research Laboratory Report ARL-TR-1565, Nov. 1997; also in *J. Mater. Res.*, 1999, vol. 14, pp 146–61.
8. D.B. Marshall, T. Noma, and A.G. Evans: *J. Am. Ceram. Soc.*, 1982, vol. 65, pp. C175–C176.
9. S.-H. Leigh, C.-K. Lin, and C.C. Berndt: *J. Am. Ceram. Soc.*, 1997, vol. 80, pp. 2093–99.
10. J.P. Singh, M. Sutaria, and M. Ferber: *Ceram. Eng. Sci. Proc.*, 1997, vol. 18, pp. 191–200.
11. H.E. Eaton, J.R. Linsey, and R.B. Dinwiddie: "The Effect of Thermal Aging on the Thermal Conductivity of Plasma Sprayed Fully Stabilized Zirconia," *Thermal Conductivity*, vol. 22, T.W. Tong, Ed.: Technomic Publishing Co., Inc., Lancaster, Pennsylvania, 1994, pp. 289–300.
12. R.B. Dinwiddie, S.C. Beecher, W.D. Porter, and B.A. Nagaraj: "The Effect of Thermal Aging on the Thermal Conductivity of Plasma Sprayed and EB-PVD Thermal Barrier Coatings," presented at The International Gas Turbine and Aeroengine Congress and Exhibition, Birmingham, UK, ASME Paper 96-GT-282, 1996.